Mechanics Research Communications 38 (2011) 274–281

Contents lists available at ScienceDirect

Mechanics Research Communications

journal homepage: www.elsevier.com/locate/mechrescom

Perturbation solution for the 2D Boussinesq equation

C.I. Christov*, J. Choudhury[1]

Dept of Mathematics, University of Louisiana at Lafayette, Lafayette, LA 70504-1010, USA

ARTICLE INFO

Article history:
Received 17 December 2009
Received in revised form 12 January 2011
Available online 21 March 2011

Keywords:
Boussinesq equation
Two-dimensional solitary waves
Perturbation method

ABSTRACT

Boussinesq equation arises in shallow water flows and in elasticity of rods and shells. It contains nonlinearity and fourth-order dispersion and has been one of the main soliton models in 1D. To find its 2D solutions, a perturbation series with respect to the small parameter $\varepsilon = c^2$ is developed in the present work, where c is the phase speed of the localized wave. Within the order $O(\varepsilon^2) = O(c^4)$, a hierarchy is derived consisting of one-dimensional fourth-order equations. The Bessel operators involved are reformulated to facilitate the creation of difference schemes for the ODEs from the hierarchy. The numerical scheme uses a special approximation for the behavioral condition in the singularity point (the origin). The results of this work show that at infinity the stationary 2D wave shape decays algebraically, rather than exponentially as in the 1D cases. The new result can be instrumental for understanding the interaction of 2D Boussinesq solitons, and for creating more efficient numerical algorithms explicitly acknowledging the asymptotic behavior of the solution.

1. Introduction

Boussinesq's equation (BE) was the first model for the propagation of surface waves over shallow inviscid fluid layer. Boussinesq (1871, 1872) developed a perturbation method to solve the Laplace equation in the bulk, and to consequently close the system that contains only the surface variable. He arrived at a generalized wave equation (GWE) that contains dispersion in addition to the standard terms. For a slowly evolving wave in a coordinate frame moving with the center of the wave, BE reduces to the Korteweg–de Vries equation which is widely studied in 1D. The approach developed by Boussinesq opened a new avenue of modeling: the 'amplitude equations'. He found an analytical solution of his equation and thus proved that the balance between the steepening effect of the nonlinearity and the flattening effect of the dispersion maintains the shape of the wave. This discovery can be properly termed 'Boussinesq paradigm'.

Apart from the significance for the shallow water flows, this paradigm is very important for understanding the particle-like behavior of nonlinear localized waves. In the 1960s it was discovered that the permanent waves can behave in many instances as particles (the so-called 'collision property'), and were called *solitons* by Zabusky and Kruskal (1965). The localized waves which can retain their identity during interaction appear to be a rather pertinent model for particles, especially if some mechanical properties (such as mass, energy, and momentum) are conserved by the governing system of equations. In 1D, a plethora of deep mathematical results have been obtained for solitons (see Ablowitz and Segur, 1981; Newell, 1985). The success was contingent upon the existence of an analytical solution of the respective nonlinear dispersive equation. As it should have been expected, most of the physical systems are not fully integrable (even in one spatial dimension) and only a numerical approach can lead to unearthing the pertinent physical mechanisms of the interactions (see, e.g., Christov and Velarde, 1994; Christov, 2001 and the literature cited therein).

The overwhelming majority of the analytical and numerical results obtained so far are for one spatial dimension, while in multidimension, much less is possible to achieve analytically, and almost nothing is known about the unsteady solutions that involve interactions, especially when the full-fledged Boussinesq equations are involved. The 2D case is relatively better studied for the so-called Kadomtsev–Petviashvili equation (KPE), which has fourth derivatives only in one of the spatial directions, while it is second-order in the other direction. Interesting analytical results are obtained for the solutions of KPE, which are localized in the direction with the fourth-order derivative, and are periodic in the other direction (see, e.g., Christov et al., 2007; Porubov et al., 2004,? and the literature cited therein).

For the time being, the 2D Boussinesq model is still less accessible analytically, which requires developing numerical techniques. The first case to undergo investigation is the steadily propagating wave profile. Some preliminary numerical results were obtained by Choudhury and Christov (2005). One of the main difficulties for the difference schemes lies in the inevitable reducing of the infinite interval to a finite one. This can be surmounted if a spectral method

* Corresponding author at: Dept. Mathematics, University of Louisiana at Lafayette, P.O. Box 1010, Lafayette, LA 70504-1010, USA. Tel.: +1 337 482 5273; fax: +1 337 482 5346.
E-mail address: christov@louisiana.edu (C.I. Christov).
[1] Current address: TeamQuest Corporation, Clear Lake, IA 50428, USA.

0093-6413/$ – see front matter © 2011 Elsevier Ltd. All rights reserved.
doi:10.1016/j.mechrescom.2011.01.014

is used with a basis system of localized functions which automatically acknowledge the requirement that the solution belongs to $L^2(-\infty, \infty)$ space. Along these lines, a specialized Galerkin spectral technique was propsed in Christov (1982), and applied to various 1D problems. Christov (1995b) created a spectral scheme for a 2D problem related to the quadratic Klein–Gordon equation (KGE). The application of the Galerkin procedure to Boussinesq model can be found in Christou and Christov (2007, 2009) for the stationary propagating 2D Boussinesq wave.

In the present work, we undertake an asymptotic semi-analytical solution for moderate phase speeds and compare the results with the above mentioned numerical works.

2. Boussinesq paradigm equation (BPE)

Following Boussinesq (1872), we restrict the derivations to the case when the shape function $h(x, y, t)$ of the free surface is single-valued, i.e., there is no wave breaking. The motion in the bulk is governed by the Laplace equation for the potential Φ. We introduce dimensionless variables according to the scheme $\Phi = UL\phi$, $h = H\eta$, $z = Hz'$, $x = Lx'$, $y = Ly'$, $t = LU^{-1}t'$, where H is the scale for the vertical spatial coordinate (the thickness of the shallow layer) and L is the wave length in the horizontal plane. Respectively, $U = \sqrt{gH}$ is the characteristic scale for the velocity. Henceforth, the primes will be omitted.

As shown in Christov (2001), the consistent implementation of the Boussinesq method yields the following generalized wave equation (GWE) for $f = \phi(x, y, 0; t)$:

$$f_{tt} + 2\beta\nabla f\cdot\nabla f_t + \beta f_t\Delta f + \frac{3\beta^2}{2}(\nabla f)^2\Delta f - \Delta f + \frac{\beta}{6}\Delta^2 f - \frac{\beta}{2}\frac{\partial^2\Delta f}{\partial t^2} = 0. \tag{1}$$

Eq. (1) is the most rigorous amplitude equation that can be derived for the surface waves over an inviscid shallow layer, when the length of the wave is considered large in comparison with the depth of the layer. Since it was derived only in 2001, it has not attracted much attention, and the plethora of different inconsistent Boussinesq equations are still vigorously investigated. Each specific simplification of the general model reveals some particular trait of the balance between the nonlinearity and dispersion. In many cases, the resulting model that is integrable (see the original Boussinesq equation containing only fourth-order spatial derivatives for the dispersion). Such a feature is clearly important for advancing the specific soliton techniques. Much has been done to compare the behavior of the solutions of the different versions of Boussinesq equations. For instance, it was shown numerically in Christov and Velarde (1994) that the soliton interactions are qualitatively very similar for the non-integrable equation with mixed fourth derivative and the original integrable Boussinesq equation. This means that some aspects of the actual physics can be captured successfully by a specific version of the Boussinesq equation. The most popular are the versions that contain a quadratic nonlinearity, and we feature the new technique proposed here for this case.

Unfortunately, Boussinesq did some additional (and as it turns out) unnecessary assumptions, which rendered his equation incorrect in the sense of Hadamard. We term the original model the 'Boussinesq's Boussinesq equation' or BBE. During the years, it was 'improved' in a number of works. An overview of the different Boussinesq equations can be found in Christov and Velarde (1994), and the literature cited therein. The mere change of the incorrect sign of the fourth derivative in BBE yields the so-called 'good' or 'proper' Boussinesq equation, which we will refer to as the Boussinesq equation or BE. A different approach to removing the incorrectness of the BBE was discussed in Benjamin et al. (1972); Bogolubsky (1977); Manoranjan et al. (1988), and the situation was remedied by changing the spatial fourth derivative to a mixed fourth derivative, which resulted into an equation know nowadays as the regularized long wave equation (RLWE) or Benjamin–Bona–Mahony equation (BBME). In fact, the mixed derivative occurs naturally in Boussinesq derivation (see Eq. (1)), and was changed by Boussinesq to a fourth spatial derivative under an assumption that $\partial_t \approx c\,\partial_x$, which is currently known as the 'linear impedance relation' (or LIA). The LIA has gained quite a currency in different fields of fluid mechanics and has produced innumerable instances of unphysical results (see Christov et al., 2007 for the case in nonlinear acoustics).

Boussinesq applied the LIA also to the nonlinear terms, and neglected the cubic nonlinearity. This simplified the nonlinear terms of Eq. (1) to a point where Boussinesq was able to find the first *sech* solution for the permanent localized wave, proving thus the existence of the balance between the nonlinearity and dispersion. The actual nonlinearity is important because it provides for the Galilean invariance of the model (see Christov, 2001). Yet for the purposes of understanding the 2D solutions, one may find it useful to stay within the Boussinesq framework of simplifications, as far as the nonlinear terms are concerned. We focus here on the following two-dimensional amplitude equation:

$$w_{tt} = \Delta\left[w - \alpha w^2 + \beta_1 w_{tt} - \beta_2\Delta w\right], \tag{2}$$

where w is the surface elevation, $\beta_1, \beta_2 > 0$ are two dispersion coefficients, and α is an amplitude parameter, which can be set equal to unity without loosing the generality. We term Eq. (2) the Boussinesq paradigm equation (or BPE). As already above mentioned, the main difference here is that BPE features one more term than BE, namely $\beta_1 \neq 0$. A note on the notation: in the original BE as related to the water waves, the nonlinear term has a positive sign, and the soltions are actually depressions for the subcritical case. Here we have deliberately changed the sign for the sake of the presentation.

It was shown in Christov (1995a, 2001) that the 1D PBE admits soliton solutions given by

$$w^s(x, t; c) = -\frac{3}{2\alpha}(c^2 - 1)\times\operatorname{sech}^2\left[\frac{1}{2}(x - ct)\sqrt{(c^2-1)/(\beta_1 c^2 - \beta_2)}\right], \tag{3}$$

where c is the phase speed. The soliton Eq. (3) is that it exists for $|c| > \max\{1, \sqrt{\beta_2/\beta_1}\}$ or $|c| < \min\{1, \sqrt{\beta_2/\beta_1}\}$. The first case is comprised by the so-called 'supercritical' solitons, while the latter encompasses the 'subritical' ones.

We set the amplitude parameter $\alpha = 1$, because it can always be eliminated by rescaling the solution. We can also select $\beta_2 = 1$. This leaves us with only one parameter, β_1, apart from the phase speed c.

For the numerical interaction of 2D Boussinesq solitons, one needs the shape of a stationary moving solitary wave in order to construct an initial condition. To this end, introduce relative coordinates $\hat{x} = x - c_1 t$, $\hat{y} = y - c_2 t$, in a frame moving with velocity (c_1, c_2). Since there is no evolution in the moving frame $v(x, y, t) = u(\hat{x}, \hat{y})$, and the following equation holds for u:

$$\begin{aligned}(c_1^2 u_{\hat{x}\hat{x}} + 2c_1c_2u_{\hat{x}\hat{y}} + c_2^2u_{\hat{y}\hat{y}}) = (u_{\hat{x}\hat{x}} + u_{\hat{y}\hat{y}}) - \left[((u^2)_{\hat{x}\hat{x}} + (u^2)_{\hat{y}\hat{y}})\right]\\ -(u_{\hat{x}\hat{x}\hat{x}\hat{x}} + 2u_{\hat{x}\hat{x}\hat{y}\hat{y}} + u_{\hat{y}\hat{y}\hat{y}\hat{y}})\\ +\beta_1\left[c_1^2(u_{\hat{x}\hat{x}\hat{x}\hat{x}} + u_{\hat{x}\hat{x}\hat{y}\hat{y}})\right.\\ +2c_1c_2(u_{\hat{x}\hat{x}\hat{x}\hat{y}} + u_{\hat{x}\hat{y}\hat{y}\hat{y}})\\ \left.+c_2^2(u_{\hat{x}\hat{x}\hat{y}\hat{y}} + u_{\hat{y}\hat{y}\hat{y}\hat{y}})\right].\end{aligned} \tag{4}$$

The so-called asymptotic boundary conditions (a.b.c.) read $u \to 0$, for $\hat{x} \to \pm\infty$, $\hat{y} \to \pm\infty$. The a.b.c.'s are invariant under rotation of the coordinate system, hence it is enough to consider solitary propagating along one of the coordinate axes, only. We chose $c_1 = 0$,

$c_2 = c \neq 0$. Without fear of confusion we will 'reset' the names of the independent variables to x, y and omit in what follows the hat over the function u.

3. Perturbation method

As above mentioned, the stationary solitary waves in the 1D case exist only for $c<1$. This sets up the limits of our scope here: $c<1$. Within this limit, we can introduce a small parameter $\varepsilon = c^2$. Even a phase speed of order of 0.5 can be considered small for the approximation purposes since it gives $\varepsilon = 0.25$. All this means, that one can attempt a perturbation solution of Eq. (4). We will restrict ourself to the case $\beta_1 = 0$. Since, it contributes to the order $O(\varepsilon)$ of the solution, then operators to be inverted are the same as for the case $\beta_1 = 0$, and only the inhomogeneous parts can change. We will present in details only the latter case in order not to overload the presentation.

The small parameter does not multiply the highest derivative, hence the expansion is regular (see, e.g., Cole, 1968). When $c = 0$, the solution possesses a radial symmetry, and we consider the expansion

$$u(x,y) = u_0(r) + \varepsilon\, u_1(x,y) + \varepsilon^2\, u_2(x,y) + \cdots, \tag{5}$$

where $r = \sqrt{x^2+y^2}$. Now, neglecting the terms of order $O(\varepsilon^3)$, we get for the three lowest orders in ε the following system

$$\frac{1}{r}\frac{d}{dr} r \frac{d}{dr}\left[u_0(r) - u_0^2(r) - \frac{1}{r}\frac{d}{dr} r \frac{du_0}{dr}\right] = 0, \tag{6a}$$

$$\varepsilon\left[\Delta(u_1 - 2u_0 u_1) - \Delta^2 u_1 - \frac{\partial^2}{\partial y^2}u_0 + \beta_1 \frac{\partial^2}{\partial y^2}(u_0 - u_0^2)\right] = 0. \tag{6b}$$

$$\varepsilon^2\left[\Delta(u_2 - u_1^2 - 2u_0 u_2) - \Delta^2 u_2 - \frac{\partial^2}{\partial y^2}u_1 + \beta_1 \Delta^2 u_2 - \frac{\partial^2}{\partial y^2}\Delta u_1\right] = 0. \tag{6c}$$

In order to avoid lengthy formulas we demonstrate in what follow the gist of the numerical approximations of the asymptotic equations for the case without the terms with β_1. Since the equations are linear the same procedure is repeated when only the terms with β_1 are retained and the final solution is a superposition of the two. We prefer to treat the above system in polar coordinates because then the region is unbounded only with respect to one of the variables (the polar radius r). The standard connection between Cartesian and polar coordinates is $x = r\cos(\theta)$, $y = r\sin(\theta)$, where θ is the polar angle. Now for the derivative with respect to y we have

$$\frac{\partial^2}{\partial y^2} \equiv \sin^2\theta \frac{\partial^2}{\partial r^2} + \frac{\cos^2\theta}{r^2}\frac{\partial^2}{\partial \theta^2} + \frac{\sin 2\theta}{r}\frac{\partial^2}{\partial r \partial \theta} - \frac{\sin 2\theta}{r^2}\frac{\partial}{\partial \theta} + \frac{\cos^2\theta}{r}\frac{\partial}{\partial r}. \tag{7}$$

The Laplace operator in polar coordinates is well known and is omitted here.

When manipulating the equation for u_1, we observe that the operator in Eq. (7) has to be applied only to the function u_0 which is independent of the polar angle θ and we get the following

$$\frac{\partial^2}{\partial y^2}u_0(r) = \sin^2\theta \frac{d^2}{dr^2}u_0(r) + \frac{\cos^2\theta}{r}\frac{d}{dr}u_0(r) = \sin^2\theta \frac{d^2F}{dr^2} + \frac{\cos^2\theta}{r}\frac{dF}{dr}.$$

Then we can recast Eqs. (6b) and (6c) as follows:

$$\left(\frac{1}{r}\frac{d}{dr} r \frac{d}{dr} + \frac{1}{r^2}\frac{\partial^2}{\partial\theta^2}\right)\left[u_1(r,\theta) - 2F(r)u_1(r,\theta) - \left(\frac{1}{r}\frac{d}{dr} r \frac{d}{dr} + \frac{1}{r^2}\frac{\partial^2}{\partial\theta^2}\right)u_1(r,\theta)\right] = \sin^2\theta \frac{d^2}{dr^2}F(r) + \frac{\cos^2\theta}{r}\frac{d}{dr}F(r) \equiv \left[\frac{1}{2}\frac{d^2}{dr^2}F(r) + \frac{1}{2r}\frac{d}{dr}F(r)\right] - \frac{\cos 2\theta}{2}\left[\frac{d^2}{dr^2}F(r) - \frac{1}{r}\frac{d}{dr}F(r)\right], \tag{8}$$

$$\left(\frac{1}{r}\frac{d}{dr} r \frac{d}{dr} + \frac{1}{r^2}\frac{\partial^2}{\partial\theta^2}\right)\left[u_2(r,\theta) - 2F(r)u_2(r,\theta) - \left(\frac{1}{r}\frac{d}{dr} r \frac{d}{dr} + \frac{1}{r^2}\frac{\partial^2}{\partial\theta^2}\right)u_2(r,\theta)\right] = \sin^2\theta \frac{\partial^2 u_1(r,\theta)}{\partial r^2} + \frac{\cos^2\theta}{r^2}\frac{\partial^2 u_1(r,\theta)}{\partial\theta^2} - \frac{\sin 2\theta}{r^2}\frac{\partial u_1(r,\theta)}{\partial\theta} + \frac{\sin 2\theta}{r}\frac{\partial^2 u_1(r,\theta)}{\partial r\partial\theta} + \frac{\cos^2\theta}{r}\frac{\partial u_1(r,\theta)}{\partial r} + \frac{\partial^2 u_1^2(r,\theta)}{\partial r^2} + \frac{1}{r}\frac{\partial u_1^2(r,\theta)}{\partial r} + \frac{1}{r^2}\frac{\partial^2 u_1^2(r,\theta)}{\partial\theta^2}. \tag{9}$$

The form of the right-hand side of Eq. (8) suggests that the following type of solution can be found

$$u_1(r,\theta) = G(r) + H(r)\cos(2\theta), \tag{10}$$

$$u_2(r,\theta) = P(r) + Q(r)\cos 2\theta + R(r)\cos 4\theta. \tag{11}$$

4. The governing system

Before proceeding with the derivation of the system for the functions F, G, H, P, Q, R we observe that the higher-order Bessel operators involved in those equations have the form:

$$\frac{d^2}{dr^2} + \frac{1}{r}\frac{d}{dr} - \frac{4}{r^2} \equiv r\frac{d}{dr}\frac{1}{r^3}\frac{d}{dr}r^2, \quad \frac{d^2}{dr^2} + \frac{1}{r}\frac{d}{dr} - \frac{16}{r^2} \equiv r^3\frac{d}{dr}\frac{1}{r^7}\frac{d}{dr}r^4, \tag{12}$$

The proof is demonstrated by simple differentiation.

We can integrate Eq. (6a) and set the two integration constants equal to zero. Thus we get a lower-order equation for $u_0(r) = F(r)$:

$$F(r) - F^2(r) - \frac{1}{r}\frac{d}{dr} r \frac{dF}{dr} = 0. \tag{13a}$$

Upon substituting Eq. (10) into Eq. (8), and integrating twice under the asymptotic boundary conditions, we get the following equation:

$$-G(r) + 2F(r)G(r) + \frac{d^2G}{dr^2} + \frac{1}{r}\frac{dG}{dr} = -\frac{1}{2}F(r). \tag{13b}$$

Implementing consistently the above idea (grouping the terms with the same dependence on θ) we get the equations for the other functions H, P, Q, R, namely:

$$r\frac{d}{dr}\frac{1}{r^3}\frac{d}{dr}r^2\left[+r\frac{d}{dr}\frac{1}{r^3}\frac{d}{dr}r^2H(r) + 2F(r)H(r) - H(r)\right] = \frac{1}{2}\left[\frac{d^2}{dr^2}F(r) - \frac{1}{r}\frac{d}{dr}F(r)\right], \tag{13c}$$

$$\frac{1}{r}\frac{d}{dr} r \frac{d}{dr}\left[-P(r) + 2F(r)P(r) + \frac{1}{r}\frac{d}{dr} r \frac{d}{dr}P(r) + (G^2 + \frac{1}{2}G - \frac{1}{4}H + \frac{1}{2}H^2)\right] = \frac{1}{2r}H', \tag{13d}$$

$$r\frac{d}{dr}\frac{1}{r^3}\frac{d}{dr}r^2\left[-Q(r) + 2F(r)Q(r) + 2GH + \frac{1}{2}H + r\frac{d}{dr}\frac{1}{r^3}\frac{d}{dr}r^2Q(r)\right] = \frac{1}{2}(G'' - \frac{1}{r}G'), \tag{13e}$$

$$r^3\frac{d}{dr}\frac{1}{r^7}\frac{d}{dr}r^4\left[r^3\frac{d}{dr}\frac{1}{r^7}\frac{d}{dr}r^4R(r)+2F(r)R(r)-R(r)+\frac{1}{2}H^2\right] = \frac{H''}{4}-\frac{5H'}{4r}+\frac{2H}{r^2}. \tag{13f}$$

When one is faced with singularities that arise from the use of specific coordinates (e.g., polar coordinates), one has to ensure the proper behavior of the functions at the point of singularity by imposing additional (purely mathematical) conditions in the geometric singularity called 'behavioral' (see Boyd, 2001). The behavioral conditions at the origin arise from the fact that there is a singularity in the operator. To ensure the sufficiently differentiable solution, one has to impose the following behavioral conditions:

$$P'(0)=P'''(0)=Q'(0)=Q'''(0)=R'(0)=R'''(0)=H'(0)=H'''(0) = G'(0)=G'''(0)=0, \tag{14a}$$

while the behavioral conditions at infinity are the asymptotic boundary conditions (a.b.c.):

$$G(r),H(r),P(r),Q(r),R(r)\to 0,\quad r\to\infty. \tag{14b}$$

The equations possess non-trivial solutions provided a nontrivial solution is found $F(r)\not\equiv 0$, because the rest of the equations are liner. Thus, one can tackle the bifurcation problem while finding the function $F(r)$.

5. Difference schemes

The boundary value problem Eqs. (13) and (14) is to be solved numerically. We use a grid which is staggered by $\frac{1}{2}h$ from the origin $r=0$, while it coincides with the "numerical infinity", $r=r_\infty$. Thus

$$r_i=(i-\frac{1}{2})h,\qquad r_{i\pm\frac{1}{2}}=r_i\pm\frac{1}{2}h,$$

where $h=r_\infty/(N-0.5)$ and N is the total number of points. The staggered grid gives a unique opportunity to create difference approximations for the Bessel operators involved in our model that take care of the singularities of the respective Bessel operator automatically, without the need to impose explicit behavioral boundary conditions in the origin. This is made possible by the fact that $r_{-\frac{1}{2}}=0$.

The crucial element in computing the function F is to obtain the nontrivial solution in a situation where the trivial solution is also present. To this end, we introduce the scaling $F(r)=\theta\hat{F}(r)$ and impose the condition $\hat{F}(0)=1$. The other boundary condition is $\hat{F}(r_\infty)=0$. The iterative procedure finds the grid function $\hat{F}_i^{n+1}$ when an approximate solution is available from the previous iteration, namely $\hat{F}_i^n$, θ^n. The finite-difference for $i=1,\ldots,N-1$ scheme reads

$$r_{i+\frac{1}{2}}\hat{F}_{i+1}^{n+1}+r_{i-\frac{1}{2}}\hat{F}_{i-1}^{n+1}-\left[r_{i-\frac{1}{2}}+r_{i+\frac{1}{2}}\right]\hat{F}_i^{n+1}-h^2r_i\hat{F}_i^{n+1}=-h^2r_i\theta^n(\hat{F}_i^n)^2, \tag{15}$$

coupled with $\hat{F}_1^{n+1}=1$, $\hat{F}_N^{n+1}=0$.

After $\hat{F}_i^{n+1}$ is computed, we find the new iteration for θ^{n+1} from the difference equation, Eq. (15). written at the point $i=1$. Here comes handy the special grid for which the value $\hat{F}_0$ is actually multiplied by $r_{-\frac{1}{2}}=0$. After applying a relaxation we get $\theta^{n+1}=\theta^n(1-\omega)-\omega[(2/h^2)\hat{F}_2^{n+1}-(1+(2/h^2))]$, where the relaxation parameter $\omega\in[0,1]$ is introduced in order to secure stability and rapid convergence of the iterations. Our numerical experiments show that $\omega\approx 0.2$ is the optimal value. After the iterations converge for certain n, the original function $F(r)$ is recovered as $\theta^{n+1}\hat{F}_i^{n+1}$. We found that $r_\infty=50$ and $N=2000$ are fully adequate for obtaining a highly accurate solution. The result is shown in Fig. 1 (solid lines). Left panel shows the linear plot, while the right panel contains log–log plots, the latter giving insight into the rate of decay of the profile at infinity. We can call the solution presented in Fig. 1 the 'radial *sech*'.

In order to verify the results, we also used a standard shooting procedure. The shooting and difference solutions are in perfect agreement in the region where the shooting is stable up to $r_\infty\approx 7$. The difference scheme gives $F(0)=2.391947$ which is in very good agreement with the shooting result of 2.39196.

We approximate Eq. (13b) in a similar fashion as the equation for $F(r)$. We can see that similarly to $F(r)$, the function $G(r)$ (dashed lines in Fig. 1) is also tightly localized. The comparison to an exponential function in the right panel of Fig. 1 shows a slightly sub-exponential decay, but what is important is that it is faster than algebraic. A conspicuous trait of $G(r)$ is that it is non-monotone. When added with the proper coefficient to $F(r)$ it may lead to a decrease in the maximal value of the profile. This effect was observed in numerical (see Choudhury and Christov, 2005) and spectral (see Christou and Christov, 2007) solutions.

For function $H(r)$, the behavioral conditions at the origin are more complicated due to the presence of the term $4r^{-2}H$. This requires that $H(0)=0$ while $r^{-1}H'$ is non-singular, i.e., $H'(0)=0$. This means that $H(r)\propto r^2$ for $r\to 0$. To enforce the additional conditions at the point of singularity, we introduce a new function, $H(r)=r^2W(r)$. Then

$$\left(\frac{d^2}{dr^2}+\frac{1}{r}\frac{d}{dr}-\frac{4}{r^2}\right)H(r)=\left(r^2\frac{d^2}{dr^2}+5r\frac{d}{dr}\right)W(r) = r^2\left[\frac{1}{r^5}\frac{d}{dr}r^5\frac{d}{dr}W(r)\right], \tag{16}$$

and we can rewrite Eq. (13c) as the following system

$$\frac{1}{r^3}\frac{d}{dr}r^5\frac{d}{dr}S(r)=\frac{1}{2}\left[\frac{d^2}{dr^2}F(r)-\frac{1}{r}\frac{d}{dr}F(r)\right],$$

$$\frac{1}{r^5}\frac{d}{dr}r^5\frac{d}{dr}W(r)-W(r)+2F(r)W(r)=S(r).$$

Apart from taking care of the two behavioral conditions in the singularity point, the new formulation allows the behavioral conditions to be satisfied because of the properties of the grid. Then

$$r_{i-\frac{1}{2}}^5S_{i-1}-\left[r_{i-\frac{1}{2}}^5+r_{i+\frac{1}{2}}^5\right]S_i+r_{i+\frac{1}{2}}^5S_{i+1}=h^2r_i^3\Gamma_i \tag{17a}$$

$$r_{i-\frac{1}{2}}^5W_{i-1}-\left[r_{i-\frac{1}{2}}^5+r_{i+\frac{1}{2}}^5\right]W_i+r_{i+\frac{1}{2}}^5W_{i+1}-h^2r_i^5W_i+2h^2r_i^5F_iW_i = h^2r_i^5S_i, \tag{17b}$$

where $\Gamma_i=(1/2)[(F_{i+1}-2F_i+F_{i-1}/h^2)-(1/r_i)(F_{i+1}-F_{i-1}/2h)]$, for $i=2,\ldots,N-1$ and $\Gamma_1=0$.

The solution for $W(r)$ (and hence $H(r)$) is not so tightly localized as is the solutions for $F(r)$, $G(r)$. This requires experimentation with the value r_∞. We have found that $r_\infty=1000$ gives a sufficient room for solution to decay properly and to satisfy the trivial conditions at infinity without distortion. Respectively, we took the number of grid points to be $N=50001$ in order to secure low truncation error of the difference scheme Eqs. (17). The shape of the computed function $H(r)$ is shown in the left panel of Fig. 2.

The right panel shows the result in log-log scale together with the comparison to a function of the type $1/r^2$. It is clearly seen that the asymptotic decay is indeed proportional to the inverse square of the polar coordinate. The right panel also testify that the 'computational infinity' $r_\infty=1000$ is fully adequate for finding $H(r)$ with good accuracy. Note that because of the exponential decay of F and

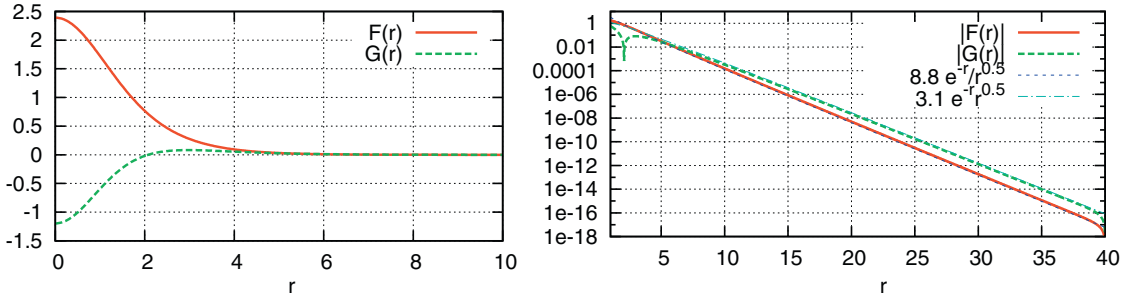

Fig. 1. The finite-difference solutions for the radial 'sech' $F(r)$ and $G(r)$. The right panel presents the same information in logarithmic coordinates and gives the best-fit exponential functions.

G we can augment the needed values of their grid versions with zeros in the region $50 < r < 100$ (outside the interval, in which F and F are computed numerically).

It is convenient to recast Eq. (13d) for $P(r)$, as the following system

$$\left(\frac{d^2}{dr^2}+\frac{1}{r}\frac{d}{dr}\right)T(r)=\frac{1}{2r}H'(r)\Rightarrow\frac{dT}{dr}=\frac{1}{2}H(r)$$

$$\Rightarrow T(r)=\int_r^\infty \frac{1}{2r}H(r), \tag{18a}$$

$$\left(\frac{d^2}{dr^2}+\frac{1}{r}\frac{d}{dr}\right)P(r)-P(r)+2F(r)P(r)$$

$$=T(r)-G^2-\frac{1}{2}G+\frac{1}{4}H-\frac{1}{2}H^2. \tag{18b}$$

Now, instead of solving a difference equation for $T(r)$ which is subject to round-off errors, we use the integrated from Eq. (18a). For the difference approximation of the indefinite integral involved, we use the trapezoidal rule which is second order in h^2, namely

$$T_i=-\frac{1}{2}\sum_{j=N}^{i+1}\frac{h}{2}\left[\frac{H_j}{r_j}+\frac{H_{j-1}}{r_j-1}\right], \tag{19}$$

which is coupled with a difference scheme for Eq. (18b) similar to the scheme for F or G.

For $r \gg 1$, we observe that $T \approx -(1/4)H$. This means that the main asymptotic behavior of order $1/r^2$ characteristic for both T and H will be canceled in the term $T(r)+(1/4)H(r)$ that enters Eq. (18b). The subtraction of two very small and almost equal numbers can introduce very large round-off errors. Hence for very large r we cannot securely assess the asymptotic order of P numerically. Immediately after the r.h.s. 'plunges' below the level of the truncation error, we are bound to get numerical noise. This is exactly what is seen in Fig. 3. Function $P(r)$ decays as $1/r^4$ for $r \leq 40$ to a value of order of 10^{-6}, but then it stabilizes there, which demonstrates the above described effect of the truncation and round-off errors. Fortunately, the magnitude of $P(r)$ in the unreliable range is so small that it does not affect the precision of the results.

In the numerical treatment of function $Q(r)$, we are guided by the same principle as in the case of function $H(r)$. Namely, we will first investigate the behavior of Q near the singular point of the operator, and then try to explicitly acknowledge this behavior in order to avoid imposing behavioral boundary conditions. Indeed, we know that $G'(0)=G'''(0)=0$, i.e., $G(r)=a-br^2+dr^4$, where, a, b, d are constants. Then $(1/2)(G''-(1/r)G')=4dr^2+O(r^4)$, i.e., the right hand side has the proper behavior needed to support the above stipulated behavior of Q. Then we can assume that $Q(r)=r^2V(r)$. Fig. 3 shows the results for $Q(r)$. It is interesting to note that, indeed, $Q(r)$ resembles $H(r)$ for large r, but has a different behavior for small r.

Concerning $R(r)$, the same arguments apply that require $R(0)=R'(0)=0$. Then we introduce a new function $R(r)=r^2Y(r)$ and rewrite Eq. (13f) as a system. We omit the details here for the sake of brevity of the presentation. The function $R(r)$ (see Fig. 3) resembles generally $H(r)$, but its contribution to the overall profile will be much smaller since it is multiplied by the second power of the small parameter.

6. Results and discussion

Because of the dependence of the 2D profile on θ, it is no longer axisymmetric for $|c| \neq 0$. We show in Fig. 4, both in linear and log–log scales, the lateral ($y=0$) and the longitudinal ($x=0$) cross-sections of the 2D profile for two different phase speeds. The profiles are also compared to numerical results obtained earlier in Choudhury and Christov (2005). The comparison is very good, which validates both the presented here semi-analytical solution and the FD solution. The advantage of the present approach is demonstrated at the boundaries of the computational box, where the FD solution deviates from the asymptotic behavior in order to

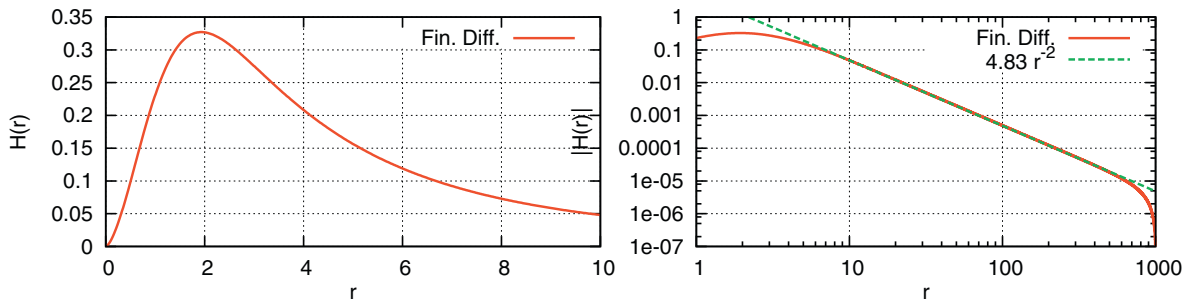

Fig. 2. Left panel: function $H(r)$. Right panel: logarithmic coordinates.

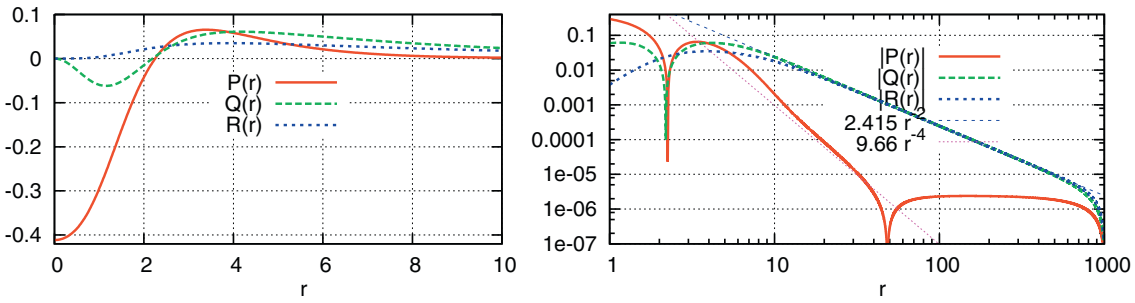

Fig. 3. Left panel: functions $P(r)$, $Q(r)$, $R(r)$. Right panel: logarithmic coordinates.

satisfy the boundary conditions on the finite domain. In the left panels, the apparent non-smooth behavior of the shapes is due to the fact that the absolute value is plotted. It is clearly seen that the first- and second-order asymptotic solution virtually coincide. Even for the case $c_1 = 0, c_2 = 0.6$ ($c_2^4 \propto 0.1$) the second-order terms do not contribute much to the profile, i.e., the first-order asymptotic solution is fully adequate. We have found that up to $|c| = 0.75$, the second-order asymptotic solution is in good quantitative agreement with the direct numerical computations which gives the limits for the applicability of the asymptotic approach developed here.

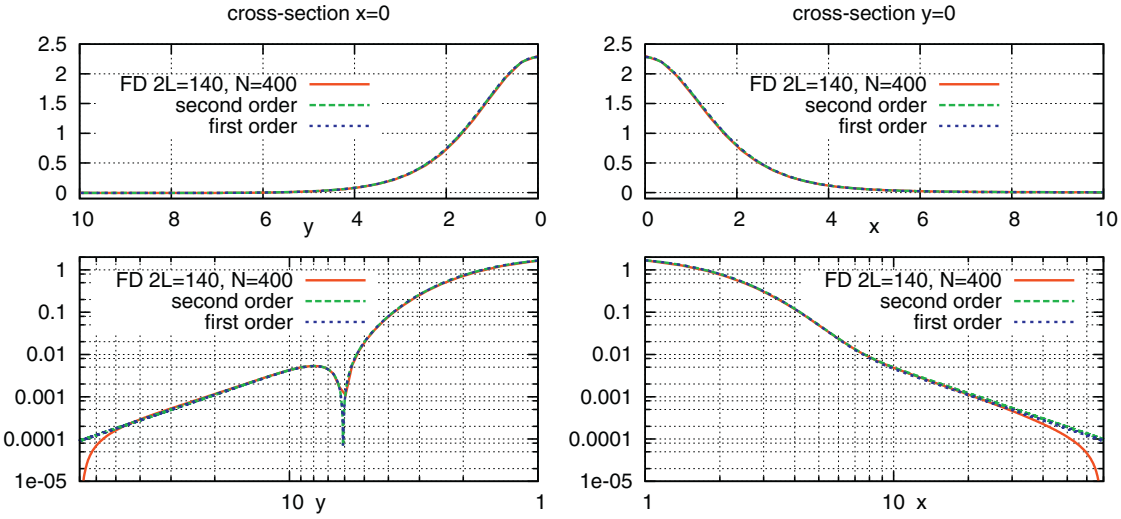

(a) Small phase speed: $c_1 = 0, c_2 = 0.3$

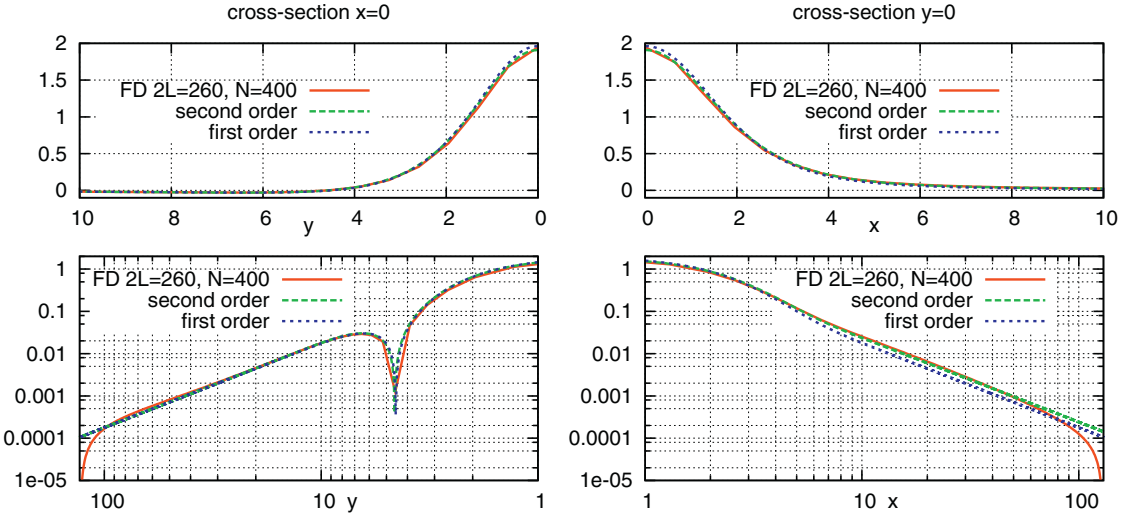

(b) Large phase speed: $c_1 = 0, c_2 = 0.6$.

Fig. 4. First- and second-order asymptotic solutions comparison to direct numerical solution: (left) longitudinal cross-section $x = 0$ and (Right) lateral cross-section $y = 0$. Solid lines: difference solution of Choudhury and Christov (2005). (a) Small phase speed: $c_1 = 0$, $c_2 = 0.3$. (b) Late phase speed: $c_1 = 0$, $c_2 = 0.3$.

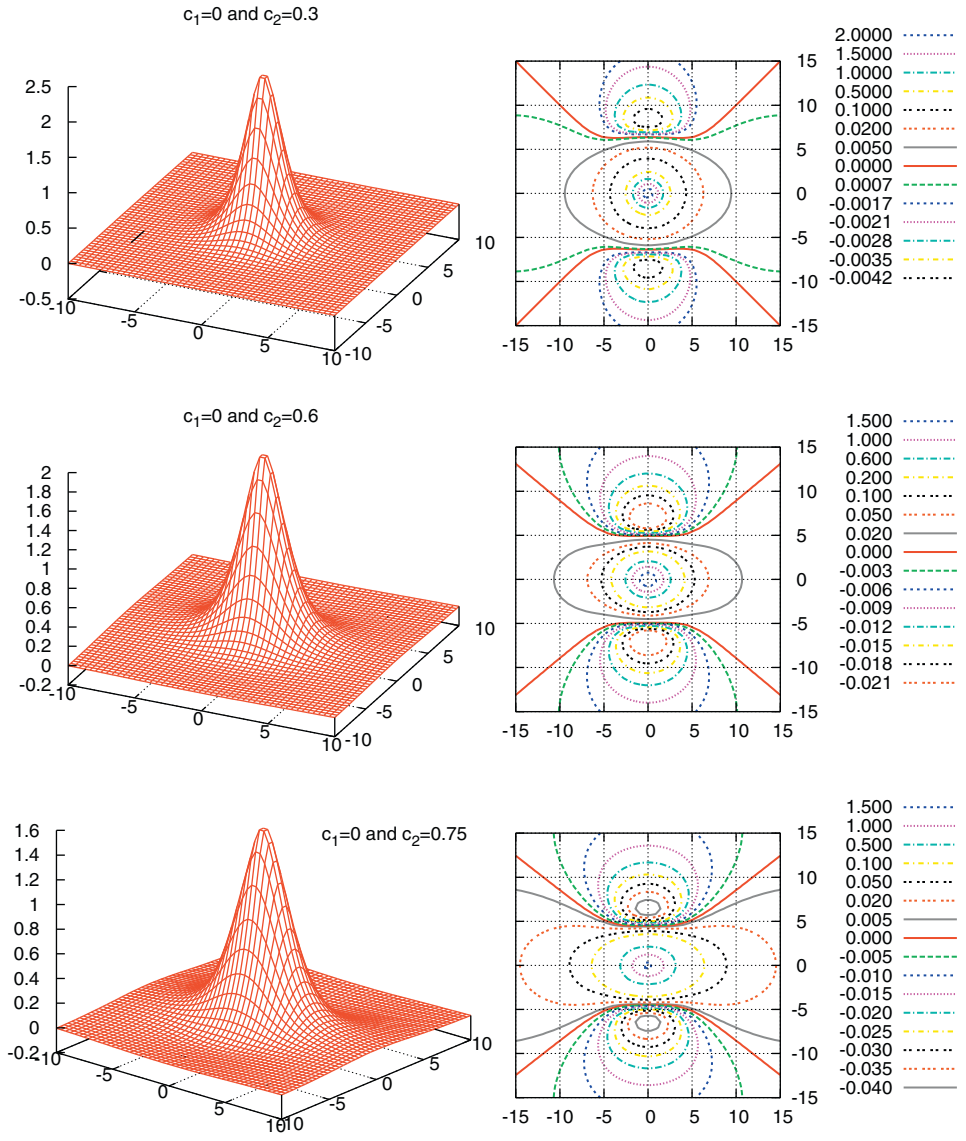

Fig. 5. The shapes of the 2D Boussinesq solitons: (left) surface plots and (right) contours.

For practical purposes, appropriate best-fit analytic expressions for the functions F, G, H, P, Q, R, can be found, and then an analytic expression can be constructed by introducing Eq. (11) into Eq. (5). As seen from the previous section, the functions involved in the u_2 term is multiplied by c^4. For the sake of providing accurate enough shape to serve as an initial condition in unsteady simulations we will keep here only terms of order of $O(c^2)$. In addition, we mention here that we repeated the above described solution procedure for $\beta_1 \neq 0$, and duly found the necessary corrections to the functions $G(r)$ and $H(r)$ stemming from the term with β_1. The final best-fit formula for $\beta_2 = 1$, reads (r, θ are the polar coordinates):

$$w^s(x,y,t;c) = f + c^2[(1-\beta_1)g_a + \beta_1 g_b] + c^2[(1-\beta_1)h_1 + \beta_1 h_2]\cos(2\theta),$$

$$f(x,y) = \frac{2.4(1+0.24r^2)}{\cosh(r)(1+0.095r^2)^{1.5}},$$

$$g_a(x,y) = -\frac{1.2(1-0.177r^{2.4})}{\cosh(r)|1+0.11r^{2.1}|},$$

$$g_b(x,y) = -\frac{1.2(1+0.22r^2)}{\cosh(r)|1+0.11r^{2.4}|},$$

$$h_i(x,y) = \frac{\sum_{j=2}^{6} a_j^i r^j}{1+\sum_{j=1}^{8} b_j^i r^j} \quad i=1,2, \tag{20}$$

The coefficients in Eq. (20) are: $a_2^1 = 1.03993$, $a_2^2 = 31.2172$, $a_3^1 = 6.80344$, $a_3^2 = -10.0834$, $a_4^1 = -0.22992$, $a_4^2 = 3.97869$, $a_5^1 = a_5^2 = 0$, $a_6^1 = 12.6069$, $a_6^2 = 77.9734$ and $b_1^1 = 13.5074$, $b_1^2 = -76.9199$, $b_2^1 = 2.46495$, $b_2^2 = 55.4646$, $b_3^1 = 2.45953$, $b_3^2 = -12.9335$, $b_4^1 = 1.03734$, $b_4^2 = 1.0351$, $b_5^1 = -0.0246084$, $b_5^2 = 0.628801$, $b_6^1 = 0.0201666$, $b_6^2 = -0.0290619$, $b_7^1 = b_7^2 = 0$, $b_8^1 = 0.00408432$, $b_8^2 = -0.00573272$. This result has already been used in numerical simulations of the unsteady propagation of Boussinesq solutions in Chertock et al. (2011).

In the end we present in Fig. 5 the two-dimensional shapes of the solitons for different values of the phase speed. In order not to overload the presentation, we set $\beta_1 = 0$. Then the only parameter that defines the shape of the soliton is the phase speed, c, since the dispersion parameter $\beta_2 = 1$. The left panels of Fig. 5 give the surface plot of the solution, while the right panels are contour plots. While the cross-section plots in Fig. 4 clearly identify the asymptotic decay of the profiles at infinity, the surface plots in Fig. 5 show the soliton

in the 'energy containing' range, where the amplitude is significant. Breaking the radial symmetry due to the translation of the solitary wave, leads to the formation of depressions in the front and the back of the wave. The depressions of negative height are well seen in the contour plots, where the spacing between the negative contours is much denser, in order to elucidate better the qualitative characteristics of the profile. This result was first observed in the numerical work (Choudhury and Christov, 2005), and is reliably confirmed here.

7. Conclusion

In the present paper we develop a perturbation technique based on the asymptotic expansion for small phase speed, c, and carry out the solution including terms up to $O(c^4)$. Within the adopted asymptotic order, we reduce the original 2D problem to six ODEs for functions that depend only on the radial variable.

We reformulate the respective Bessel operators in the so-called 'divergent' form, and create difference schemes that automatically account for the 'behavioral' boundary conditions in the origin of the coordinate system and at infinity. The results are in very good quantitative agreement in the energy-containing region with the direct difference solutions and spectral solutions. We summarize the comprehensive semi-analytical/semi-numercial solutions as best-fit functions of the governing parameters.

Our results show that the asymptotic decay of the wave profile is algebraic rather than exponential (as it is the case with the axisymmetric profile of the standing 2D soliton). This means that the 2D shape is not robust: even the presence of a very small phase speed changes qualitatively the behavior of the shape in the far field.

The new results are of importance both for the mathematical theory of Boussinesq solitons in multi-dimension, and for their physical applications, because the interaction of the solitons is determined by their shapes at large distances.

References

Ablowitz, M.J., Segur, H., 1981. Solitons and the Inverse Scattering Transform. SIAM, Philadelphia.

Benjamin, T.B., Bona, J.L., Mahony, J.J., 1972. Model equation for long waves in nonlinear dispersive systems. Philos. Trans. R. Soc. Lond. A272, 47–78.

Bogolubsky, I.I., 1977. Some examples of inelastic soliton interactions. Comput. Phys. Commun. 13, 149–155.

Boussinesq, J.V., 1871. Théorie générale des mouvements qui sont propagés dans un canal rectangulaire horizontal. Comp. Rend. Hebd. des Seances de l'Acad. des Sci. 73, 256–260.

Boussinesq, J.V., 1872. Théorie des ondes et des remous qui se propagent le long d'un canal rectangulaire horizontal, en communiquant au liquide contenu dans ce canal des vitesses sensiblement pareilles de la surface au fond. Journal de Mathématiques Pures et Appliquées 17, 55–108.

Boyd, J.P., 2001. Chebishev and Fourier Spectral Methods, 2nd ed. Dover, New York.

Chertock, A., Christov, C.I., Kurganov, A., 2011. Central-upwind schemes for the Boussinesq paradigm equation. In: Proceedings of the 4th Russian–German Advanced Research Workshop on Computational Science and High Performance Computing. In: E. Krause et al. (Eds.): Computational Sci., & High Performance Computing IV, NNFM 115, Springer-Verlag Berlin Heidelberg, pp. 267–281.

Choudhury, J., Christov, C.I., 2005. 2D solitary waves of Boussinesq equation. In: ISIS International Symposium on Interdisciplinary Science, Natchitoches, October 6–8, 2004, APS Conference Proceedings 755, Washington, DC, pp. 85–90.

Christou, M.A., Christov, C.I., 2007. Fourier–Galerkin method for 2D solitons of Boussinesq equation. Math. Comput. Simul. 74, 82–92.

Christou, M.A., Christov, C.I., 2009. Galerkin spectral method for the 2D solitary waves of Boussinesq paradigm equation. In: AIP Conf. Proc., Vol. 1186 , pp. 217–225.

Christov, C.I., 1982. A complete orthonormal sequence of functions in $L^2(-\infty\ \infty)$ space. SIAM J. Appl. Math. 42, 1337–1344.

Christov, C.I., 1995a. Conservative difference scheme for Boussinesq model of surface waves. In: W.K. Morton, M.J. Baines (Eds.), Proc. ICFD V, Oxford University Press, pp. 343–349.

Christov, C.I., 1995b. Fourier–Galerkin algorithm for 2D localized solutions. Annuaire de l'Univ. Sofia, Livre 2 – Mathématiques Appliqee et Informatique 89, 169–179.

Christov, C.I., 2001. An energy-consistent Galilean-invariant dispersive shallow-water model. Wave Motion 34, 161–174.

Christov, C.I., Maugin, G.A., Porubov, A., 2007. On Boussinesq's paradigm in nonlinear wave propagation. C. R. Mecanique 335, 521–535.

Christov, C.I., Velarde, M.G., 1994. Inelastic interaction of Boussinesq solitons. J. Bifurcat. Chaos 4, 1095–1112.

Christov, I., Christov, C.I., Jordan, P.M., 2007. Modeling weakly nonlinear acoustic wave propagation. Q. J. Mech. Appl. Math. 60 (4), 473–495.

Cole, J.D., 1968. Perturbation Methods in Applied Mathematics. Blaisdell Pub. Co., Waltham.

Manoranjan, V., Ortega, Sanz-Serna, J.M., 1988. Soliton and antisoliton interactions in the good Boussinesq equation. J. Math. Phys. 29, 1964–1968.

Newell, A.C., 1985. Solitons in Mathematics and Physics. SIAM, Philadelphia.

Porubov, A.V., Maugin, G.A., Mateev, V.V., 2004. Localization of two-dimensional non-linear strain waves in a plate. Nonlinear Mech. 39, 1359–1370.

Porubov, A.V., Pastrone, F., Maugin, G.A., 2004. Selection of two-dimensional nonlinear strain waves in micro-structured media. C. R. Mecanique 332, 513–518.

Zabusky, N.J., Kruskal, M.D., 1965. Interaction of 'solitons' in collisionless plasma and the recurrence of initial states. Phys. Rev. Lett. 15, 240–243.